International Symposium on New Developments in Advanced High-Strength Sheet Steels
19–22 June 2023, Vail, Colo., USA
DOI: 10.33313/298/010

# Evaluation of Aging and Zn-Coating Effects on Sheared Edge Formability in Sheet Steels

A. Carley-Clopton[1], K.O. Findley[1], E. De Moor[1], R.J. Comstock[2]

[1]Advanced Steel Processing and Products Research Center
Colorado School of Mines
1500 Illinois St, Golden, CO 80401

[2]Cleveland-Cliffs Steel Corp.
6180 Research Way, Middletown, OH 45005

## ABSTRACT

Sheared edge ductility is critical for formed advanced high strength steel parts. Previous studies have found that hole expansion ratio (HER) decreases with room temperature aging for a variety of steel grades. The current study examines this phenomenon in five grades of sheet steel with various strength levels and microstructures. Additionally, the effect of a hot-dip Zn coating was evaluated using a DP800 steel annealed at different dew points and then hot dip galvanized or left in the bare condition. Hole expansion testing was conducted immediately after blanking and for aging times between 15 min and 240 h at -15 °C, 21 °C, and 49 °C. A decrease in HER was observed in a complex phase, martensitic, and one dual phase grade. The effect was absent in bake hardening, transformation induced plasticity aided bainitic-ferritic, and the other of the dual phase grades. Elevated temperature aging of the complex phase grade led to an acceleration of the loss of HER and an eventual recovery of HER at long aging times. The Zn coated DP800 exhibited a greater loss in HER than the bare condition.

## INTRODUCTION

Advanced high strength steels (AHSS) are increasingly being used in the automotive industry to decrease vehicle weight and improve crashworthiness [1]. These increases in performance are made possible by the retention of the high global formability required to make parts with complex geometries at higher strength levels. In the forming of sheet metal parts, there is often stretching of sheared edges made when parts are blanked from a larger sheet or coil, making the local formability of sheared edges of critical importance in the production of sheet steel parts. Hole expansion testing (HET) is designed to evaluate the stretch flangeability of sheet steels by expanding a punched hole until a crack forms through the material thickness [2]. The hole expansion ratio (HER) is defined by Equation (1), where $D_i$ is the diameter of the hole before testing and $D_f$ is the diameter of the hole at the formation of a through thickness crack.

$$HER = \frac{D_f - D_i}{D_i} \tag{1}$$

When specimens are blanked for HET, time passes between blanking and testing, which can be anywhere between minutes and days. Previous studies have found that this delay, which will be referred to as "aging time," can decrease the measured HER value [3–5]. A study by Stewart and Comstock [3] found a noticeable decrease in HER with aging time for dual phase (DP), complex phase (CP), and high strength low alloy (HSLA) grades. A study by Atzema and Seda [4] found that for a DP 800 material, aging between blanking and testing caused a significant decrease in HER for a Zn coated condition, but not for a bare condition. A similar finding was made by Winzer *et al.* [5] for DP grades of several different strength levels.

Two proposed explanations for this behavior are static strain aging [3] and hydrogen embrittlement [4,5]. Static strain aging is a phenomenon whereby an increase in yield strength and yield point elongation are brought about by plastic strain in the material followed by aging, typically at an elevated temperature. Static strain aging is caused by interstitial solute atoms diffusing to dislocation cores to relieve elastic strain energy, leading to dislocation pinning [6]. Since punching a hole in sheet material causes plastic strain, the conditions for strain aging in the sheared edge might be met when accompanied with time for the aging to occur. Strain aging often produces an increase in yield strength (YS) and ultimate tensile strength (UTS), both of which often correlate to a decrease in HER [7].

Hydrogen embrittlement is the phenomenon by which the presence of dissolved hydrogen in steel leads to a decrease in ductility. Possible sources of hydrogen in the sheared edge are the atmosphere in which the material is aged and internal hydrogen diffusion to the sheared edge. The high strength of AHSS enhances susceptibility to hydrogen embrittlement [8]. It has been shown that hydrogen in pre-charged specimens preferentially moves to the area surrounding the sheared edge over time [5]. It follows that diffusion of that hydrogen to the strained region near the sheared edge could lead to a local loss of ductility and corresponding decrease in HER. It has been found that the threshold stress for hydrogen induced stress corrosion cracking is reduced in Zn coated punched hole tensile specimens submerged in a NaCl solution when compared to bare specimens submerged in the same solution. It was proposed that the galvanic couple formed by the steel and Zn leads to the electrochemical reduction of hydrogen from solution, which enables H-charging of the sheared edge [9]. Hydrogen charging via galvanic corrosion, even in an air atmosphere, could be another possible explanation for the aging effect on hole expansion ratio.

This study aims to isolate the effects of different variables related to both static strain aging and hydrogen embrittlement through 1) examining grades with differing sensitivities to strain aging and hydrogen embrittlement and 2) evaluating a bare and coated grade subjected to comparable environmental and thermal histories.

## METHODS

### Materials

Two of the materials used by Stewart and Comstock, DP 780 and CP 780 [3], were used in this study. A bake hardening (BH) grade, BH 210, was chosen as well since BH grades are very ductile, but exhibit static strain aging due to the presence of interstitial solute [10]. A cold rolled martensitic (CRM) 1500 grade was chosen because martensitic grades of that strength level are sensitive to hydrogen embrittlement [8], and it is a high strength grade that lacks interfaces between hard and soft phases, which can serve as initiation points for sheared edge fracture [11]. A transformation induced plasticity (TRIP) aided bainitic ferritic (TBF) 1200 grade was chosen in order to characterize the aging response of a third generation AHSS containing retained austenite. In order to investigate the effects of Zn coating, DP 800 from Tata Steel Europe was also used, produced in a simulator to be either bare or hot dip galvanized with a dewpoint of either -10 °C or -50 °C. Previous studies comparing bare and Zn coated steel have used material produced on different lines [4] or removed the Zn from coated material to produce the bare condition [5]. By using the same steel alloy annealed and coated in a simulator, this study aims to isolate the effects of coating and annealing atmosphere. Annealing atmosphere dewpoint controls the oxidation behavior of steel and affects Zn wettability [12]. As the dewpoint used to produce bare and Zn coated material may differ, a low dewpoint (-50 °C) and high dewpoint (-10 °C) were chosen to investigate whether the difference in behavior between bare and Zn coated material was due to the coating or the annealing atmosphere. Compositions, thicknesses, and coating conditions for the alloys are shown in Table I.

Tensile testing was conducted according to the ASTM E8 (full size) standard [15]. A crosshead displacement rate of 0.1 mm $s^{-1}$ (0.24 in $min^{-1}$) was used to achieve an engineering strain rate of 0.001 $s^{-1}$ for the 102 mm (4 in) gauge length of the specimens. Axial strain was measured with an extensometer. Specimens were produced by waterjet cutting and were oriented parallel to the rolling direction of the sheet. Four specimens for each grade were tested.

### Characterization

Micrographs were taken using light optical microscopy (LOM). Samples were mounted to examine a plane containing the rolling and normal directions. Samples were polished in a progression finishing with 1 μm polishing media and were then etched with 2 pct nital (2 pct nitric acid, 98 pct methanol by volume).

The H content was measured using 1 $\pm$ 0.1g samples in a LECO® OHN gas analyzer. For each condition, 10 measurements were taken. Before measuring, calibration was performed with a blank (tin flux with no sample) as well as a LECO® hydrogen in steel standard with 2.2 $\pm$ 0.5 ppm H.

Table I – Chemistry of Steel Grades Used in this Study (wt pct)

| | Thickness (mm) | Coating | C | Mn | Si | Ni | Cr | Mo |
|---|---|---|---|---|---|---|---|---|
| DP 780 | 1.50 | GI | 0.09 | 2.14 | 0.29 | N/R | 0.20 | 0.11 |
| CP 780 | 1.60 | GI | 0.11 | 1.81 | 0.24 | N/R | 0.24 | 0.16 |
| BH 210 | 0.81 | GI | 0.01 | 0.46 | 0.01 | N/R | 0.04 | 0.02 |
| CRM 1500 | 1.60 | Bare | 0.21 | 1.03 | 0.20 | 0.04 | 0.03 | 0.00 |

| | | | | | | | | |
|---|---|---|---|---|---|---|---|---|
| TBF 1200 | 1.56 | Bare | 0.20 | 2.51 | 1.51 | 0.03 | 0.05 | 0.01 |
| DP 800 | 1.58 | Bare/GI | 0.14 | 2.14 | 0.20 | - | 0.25 | - |

| | Ti | Nb | Al | S | P | Cu |
|---|---|---|---|---|---|---|
| DP780 | - | 0.02 | 0.038 | 0.006 | 0.020 | - |
| CP780 | 0.02 | 0.04 | 0.059 | 0.003 | 0.007 | - |
| BH 210 | - | - | 0.028 | 0.011 | 0.047 | - |
| CRM1500 | 0.03 | - | 0.03 | 0.003 | 0.01 | 0.15 |
| TBF1200 | 0.00 | 0.00 | 0.04 | 0.00 | 0.01 | 0.02 |
| DP 800 | 0.004 | 0.02 | 0.05 | <0.001 | 0.01 | - |

## RESULTS

### Tensile Properties

Representative engineering stress-strain behavior is shown in Figure 1 for the five grades compared in the 1 h – 10 d study. The grades represent a wide range of strength and total elongation values, with the BH 210 having the lowest UTS at 349 MPa and highest total elongation (TE) at 40.2 pct, while the CRM had the highest UTS of 1635 MPa and lowest TE of 6.8 pct. Both the CP 780 and BH 210 exhibited yield point phenomena, while the CRM 1500, TBF 1200, and DP 780 all exhibited continuous yielding behavior. Tensile properties are tabulated in Table II along with the HER value with no aging for each grade, with each property being the mean value of four tests.

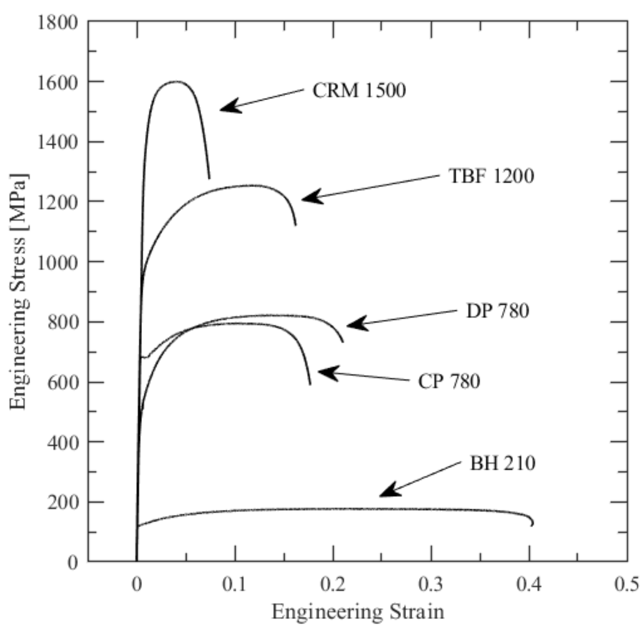


Figure 1. As received engineering stress-strain curves for representative samples of CRM 1500, TBF 1200, DP 780, CP 780, and BH 210 tested parallel to the rolling direction.

Table II – Tensile Properties for the Studied Grades

| Grade | YS [MPa] | UTS [MPa] | UE [pct] | TE [pct] | HER With no Aging [pct] |
|---|---|---|---|---|---|
| DP 780 | 508 | 823 | 13.8 | 20.8 | 19 |
| CP 780 | 682 | 793 | 11.2 | 18.5 | 56 |
| BH 210 | 242 | 349 | 20.3 | 40.2 | 122 |
| CRM 1500 | 1368 | 1635 | 3.8 | 6.8 | 46 |
| TBF 1200 | 947 | 1255 | 8.6 | 16.0 | 20 |

 

**Optical Microscopy**

Micrographs of the cross section of sheared edges of DP 780, CP 780, BH 210, CRM 1500, and TBF 1200 are shown in **Error! Reference source not found.**. The grades examined have various sheared edge morphologies, with CRM 1500 and TBF 1200 both having short rollover and burnished regions and long fracture regions, the BH 210 having a short fracture region with more rollover and burnish, and the DP 780 and CP 780 falling in between those extremes. In general, the grades with higher strengths have a longer fracture region relative to the sheet thickness.

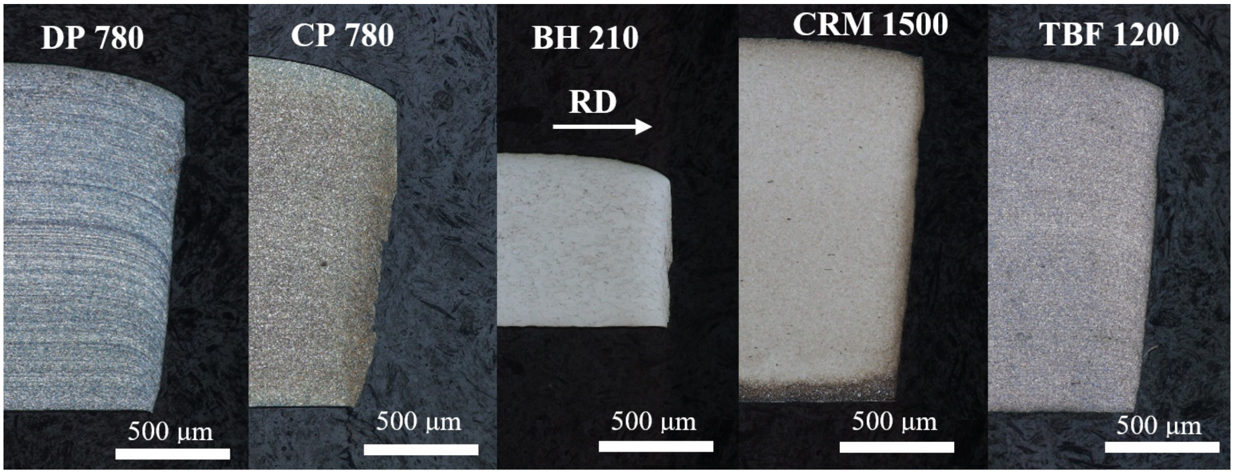


(a) (b) (c) (d) (e)

Figure 2. LOM micrographs of sheared edges for (a) DP 780, (b) CP 780, (c) BH 210, (d) CRM 1500, and (e) TBF 1200 mounted such that the sheared edge surfaces are normal to the rolling direction. Samples were polished to 1 µm then etched with 2 pct nital (2 pct nitric acid, 98 pct methanol by volume).

**Hole Expansion**

In order to examine the effect of room temperature aging between blanking and testing, specimens of five grades were tested immediately after punching the hole (approximately 1 min) as well as with aging times of 1.5 h, 4 h, 6 h, 24 h, 48 h, 96 h, and 240 h. The average and maximum and minimum of HER of those specimens is plotted against aging time in Figure 3. The BH 210 had the highest initial HER and exhibited no loss in HER with aging. The CP 780 and CRM 1500 had similar initial HER values and both exhibited a similar drop in HER with increased aging time at room temperature. The DP 780 and TBF 1200 both had low initial HER values and did not exhibit a drop in HER with increasing aging time. The relatively low values and high scatter in the data for those grades makes it difficult to interpret aging effects.

Comparison of the HET data for the room temperature aging of CP 780 to aging at a slightly elevated temperature of 49 °C and in a freezer at -15 °C is shown in Figure 4. It is clear that the decrease in HER occurs at shorter times at an elevated temperature than at room temperature and that specimens stored in a freezer exhibited less of a change in HER than specimens stored at room temperature. To compare different time and temperature combinations, a tempering parameter was used. This parameter, shown in Equation (2) has been used to compare bake hardening parameters of AHSS [16]. When compared in this way, there is fairly close agreement between the two data sets. One notable difference is that at the highest aging time for the elevated temperature aging, there appears to be a restoration of the HER to near the initial value, highlighted in Figure 4 (b) with a dashed box.

$$Tempering\ Parameter = T[11.8 + \log(t)] \quad (2)$$

 

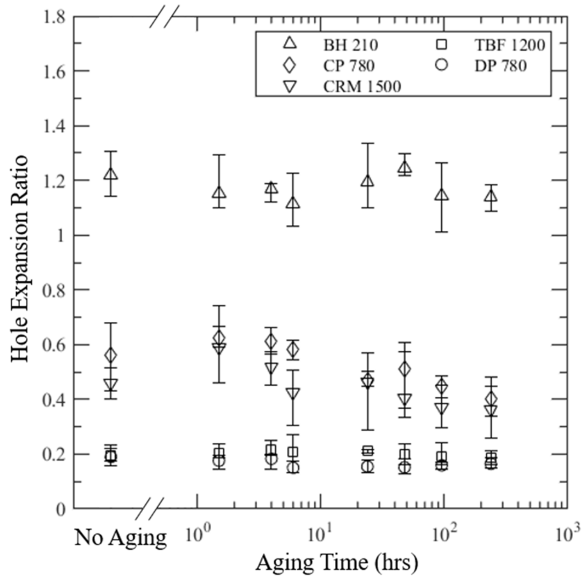


Figure 3. HER after 90 minutes to 10 days of delay between blanking and testing at room temperature for CRM 1500, TBF 1200, DP 780, CP 780, and BH 210. Each data point is the average of four replicates with the error bars showing the maximum and minimum of the replicates. Values for samples with no aging time are shown to the left.

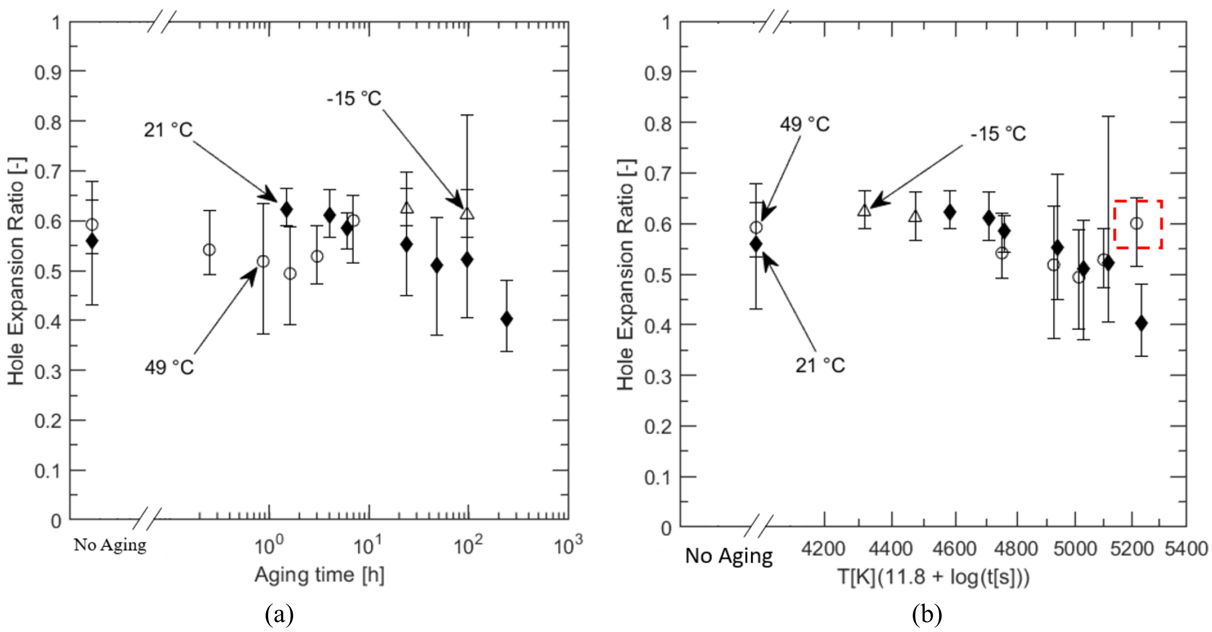


Figure 4. HER for CP 780 plotted against (a) aging time and (b) tempering parameter used to compare bake hardening parameters of AHSS [16] for specimens aged at 21 °C and 49 °C. Each point is the average of four replicates, and the error bars show the maximum and minimum values. Values for samples with no aging time are shown to the left. In (b) the condition at elevated temperature which showed a clear recovery of HER is highlighted with a dashed box.

**3.4 HER Aging Comparison Between Bare and GI DP 800**

As several studies have found a connection between the presence of a Zn coating and loss of HER with aging [4,5], a comparison was conducted using DP 800 specimens which had either been hot-dip galvanized in a galvanizing/annealing simulator, or given the same thermal history without dipping in a Zn bath. In order to isolate the effects of coating and annealing atmosphere, two annealing atmosphere dewpoints were examined. A higher dewpoint shifts oxidation from external to internal and is often used in the production of galvanized (GI) steel as this transition improves Zn adhesion [17]. The aim of using a high and low dewpoint is to determine whether the differences in aging behavior examined in bare and GI steel [4] were due to the coating or the different furnace atmospheres used. The results for samples tested immediately after punching and blanking and after 96 h of room temperature aging are shown in Figure 5. For both dewpoints, there was a clear decrease in HER with aging for the GI condition, but there is no clear change in HER in the bare condition. All four conditions had very similar starting HER, which differs from findings in previous studies examining aging effects on HER, where the GI material started with a significantly higher HER than the bare material [4] [5]. The similarity of the starting HER for this material suggests that HER differences in previous studies between bare and GI material may have been due to factors other than the coating itself.

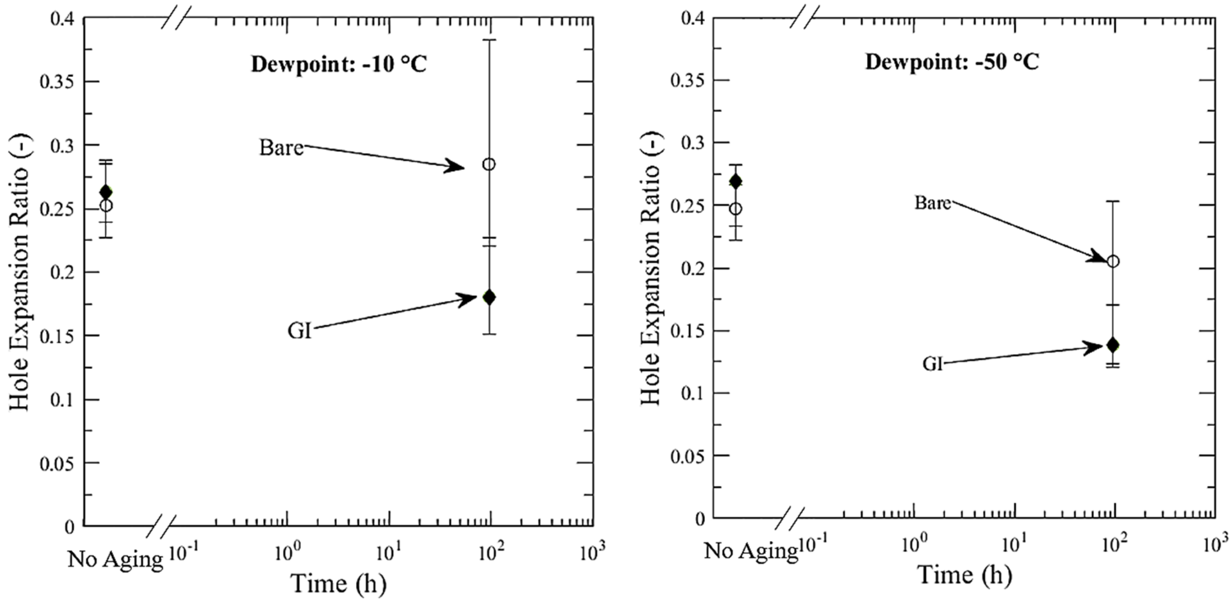


(a) (b)

Figure 5. HER for bare and GI DP 800 specimens tested immediately after punching and blanking and after 96 h of aging with annealing atmosphere dewpoints of -10 °C (a) and -50 °C (b). Each data point is the average of four replicates with the error bars showing the maximum and minimum of the replicates. Values for samples with no aging time are shown to the left.

## DISCUSSION

The following section discusses the relationship between HER and tensile properties and sheared edge formability, which is followed by a consideration of potential strain aging and hydrogen embrittlement effects based on the results presented in the previous section.

### Tensile Properties and Sheared Edge Morphology

In the grades examined, the HER and decrease of HER with aging was not correlated with tensile properties nor sheared edge morphology. Although it has generally been found that HER has a negative correlation with YS and UTS [7], this correlation was not present across the grades examined in this study. The DP 780, for example, has a much lower YS and UTS than the CRM 1500, but also had a lower initial HER value. The low HER value of the DP 780 may be due to strain incompatibility between ferrite and martensite leading to the growth of cracks in the sheared edge during HET [11]. There is no clear relationship between the tensile properties of a given grade and susceptibility to decreases in HER with aging. The two most susceptible grades, CP 780 and CRM 1500, had significant differences in strength and total elongation; and while the DP 780 and CP 780 had similar tensile properties, only the latter exhibited a significant aging response. Additionally, the relative size of the sheared edge features in these materials did not correspond to either the initial HER or the effect of aging on HER.

### Strain Aging

Some of the findings in this study are consistent with strain aging as the responsible mechanism for a reduction in HER with aging, while other results would not be well explained by strain aging. As shown in Figure 4, the acceleration of the aging effect with elevated temperature along with the relative agreement between the two aging temperatures when compared with tempering parameter suggests that a thermally activated process is operative; this observation could support either strain aging or hydrogen embrittlement as mechanisms responsible for the drop in HER. Thus, an approximation of the bulk diffusion distance of both carbon and hydrogen was calculated for each of the aging conditions using Equation (3), where $d$ is the root mean square (RMS) displacement, $D$ is a temperature dependent diffusivity, and $t$ is time; the results are shown in Figure 6 as

HER plotted against bulk diffusion distance of either carbon or hydrogen. The diffusivity is calculated in Equation (4), where $D_0$ is a constant for each element, $Q$ is the activation energy for diffusion, $R$ is the ideal molar gas constant (8.314 J $mol^{-1}$ $K^{-1}$), and $T$ is the temperature. Each point represents a time-temperature combination used in this study. The plots show that for the temperature range examined, the RMS diffusion distance for carbon better correlates to the HER for specimens aged at different temperatures than that of hydrogen does. This analysis suggests that the either 1) the bulk diffusion of carbon is associated with the reduction of HER through a thermally-dependent mechanism, consistent with the correlation to tempering parameter shown in Figure 4, or 2) that if hydrogen embrittlement is the primary mechanism reducing edge ductility, then the bulk diffusion of hydrogen does not dictate the degree of ductility loss.

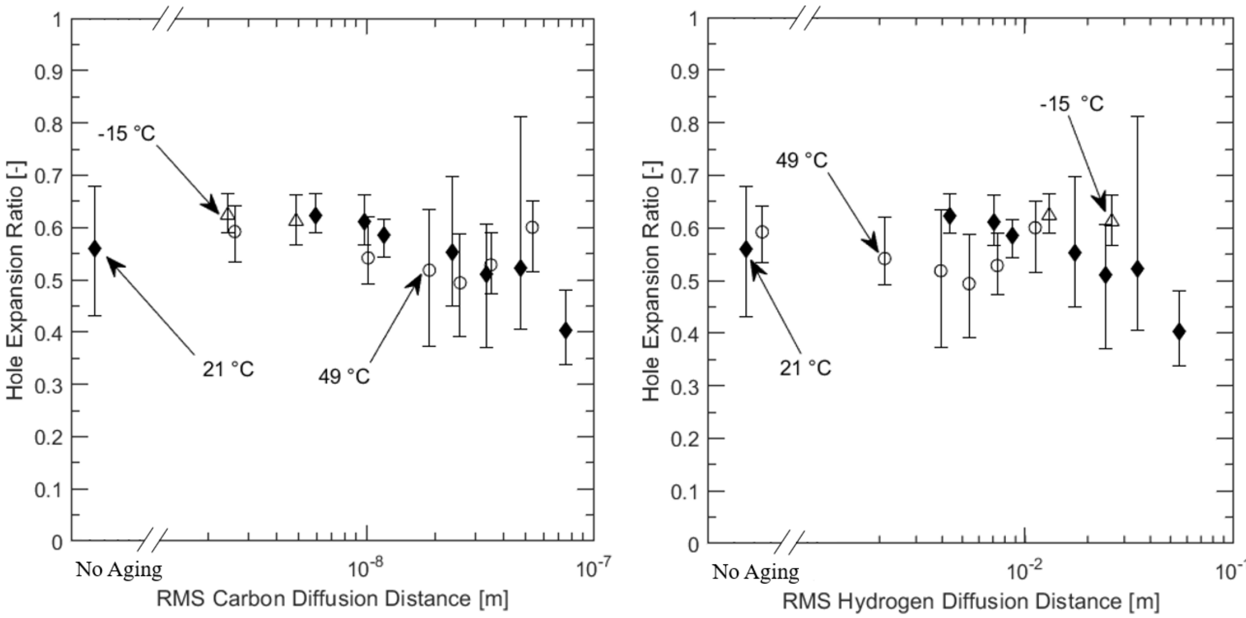


(a) (b)

Figure 6. Root mean square (RMS) diffusion distance plotted against tempering parameter for (a) carbon and (b) hydrogen. The time-temperature combinations represent those used for the hole expansion testing conducted for this study, and the RMS displacement is a calculated value.

Several findings would not be well explained by strain aging as the primary mechanism. The BH 210, with by far the highest HER, did not exhibit an aging effect in the present study. This result suggests that strain aging capacity alone is not sufficient to cause a loss of HER with aging. Additionally, in the elevated temperature study performed on the CP 780 grade, the HER of the condition aged for the longest time is nearly restored to the initial value, while the HER of the conditions aged at room temperature to a comparable tempering parameter continued to decline. This observation does not support strain aging as the responsible mechanism, as strain aging would be expected to produce an increase in YS and UTS with additional aging time at an elevated aging temperature, leading to a reduced HER. It was also found that bare DP 800 did not exhibit an aging effect while Zn coated DP 800 did. These data also suggest that static strain aging is not a sufficient explanation for the decrease in HER as the static strain aging response should not be affected by the coating.

$$d = \sqrt{Dt} \quad (3)$$

$$D = D_0\, e^{-\frac{Q}{RT}} \quad (4)$$

| | | |
|---|---|---|
| **Carbon:** | $D_0 = 0.0039\ cm^2\ s^{-1}$ | |
| | $Q = 80.2\ kJ\ mol^{-1}$ | [18] |
| **Hydrogen**: | $D_0 = 0.00075\ cm^2\ s^{-1}$ | |
| | $Q = 10.1\ kJ\ mol^{-1}$ | [18] |

**Hydrogen Embrittlement**

In addition to the results not sufficiently ascribed to strain aging, some of the findings in this study are possibly explained by hydrogen embrittlement. These include the performance of specimens aged for 7 h at elevated temperature, the results from the study of bare and coated DP 800, and the effects of aging on the HER of BH 210 and CRM 1500.

 

The recovery of HER after longer aging times at elevated temperature in the CP 780 grade may indicate the importance of hydrogen embrittlement in the aging effects. Hydrogen can gather at trap sites with an associated binding energy, one of the parameters considered when evaluating the movement of hydrogen in steel [5]. It is possible the elevated aging temperature allows hydrogen to be released from low energy trap sites and leave the alloy, reducing the extent of hydrogen embrittlement in the sheared edge and restoring edge ductility. For the CP 780, hydrogen measurements were taken from the as received condition (effectively aged for months at room temperature) and specimens which were aged at 49 °C for 7 h, to mimic the condition which led to increased HER when compared to room temperature aging. The results are shown in Figure 7. Although there is overlap of the measured values for both conditions, the condition aged at elevated temperature has a lower average and maximum hydrogen content. This finding suggests that the increase in HER after longer aging times at elevated temperature may be due to a reduction of the amount of hydrogen in the alloy.

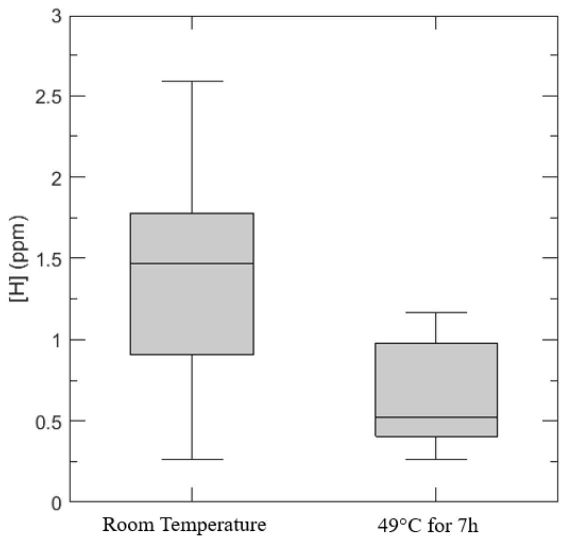


Figure 7. Measured hydrogen concentration in CP 780 specimens as received and stored at room temperature and after aging for 7 h at 49 °C. H content was measured using a LECO® OHN gas analyzer, and 10 specimens for each condition were measured.

The HET results of DP 800 produced in an annealing and galvanizing simulator suggest that a Zn coating influences the effect of aging on sheared edge ductility, as the process for producing these specimens eliminates potential confounding variables including composition, thermal history, annealing atmosphere, and hydrogen introduction through pickling. The presence of a coating may increase the hydrogen concentration of the steel by preventing the escape of readily diffusible hydrogen [5]. The pronounced reduction of HER with aging of the bare CRM 1500 suggests that a coating is not necessary for a material to lose edge ductility with time. However, martensitic grades with similar tensile properties have been shown to lose significant amounts of ductility with hydrogen charging [19], suggesting that a hydrogen effect may still be relevant. Hydrogen embrittlement as the primary mechanism may explain the lack of a significant aging response from the BH 210, as lower strength alloys are typically less sensitive to hydrogen embrittlement [8].

## CONCLUSIONS

This study investigated the HER of a variety of steel grades and evaluated the effects of aging time, aging temperature, and the presence of a Zn coating. The following conclusions are interpreted from the HER aging results in this study:

1. Neither tensile properties nor sheared edge morphology were predictive of whether a steel grade is sensitive to a reduction in HER after aging.
2. The presence of a Zn coating was found to elicit a loss of HER with aging in a DP 800 grade compared to the bare condition of the same grade; however, a Zn coating is not a necessary condition for a steel to exhibit a loss in HER with aging, as demonstrated by the bare CRM 1500 HER results. Both of these results may be explained by the potentially higher hydrogen embrittlement susceptibility in the coated DP 800 and CRM 1500 conditions.
3. The HER reduction at different aging temperatures is similar when compared via a tempering parameter, suggesting a thermally activated mechanism is responsible. The HER values for specimens aged at different temperatures correlate more closely when plotted against the calculated RMS diffusion of bulk carbon than of hydrogen, which

 

supports strain aging as a potential mechanism responsible for the HER reduction. A notable exception to this observation is the recovery of some edge ductility at longer aging times at 49 °C, possibly due to the reduction of bulk H content as measured in specimens aged for 7 h at 49 °C in comparison to the H content of specimens made from as received material.


## ACKNOWLEDGEMENTS

The authors gratefully acknowledge the support of the sponsors of the Advanced Steel Processing and Products Research Center, an industry/university cooperative research center at the Colorado School of Mines. Particularly, the authors would also like to thank D. Hanlon, E. Atzema, and M. Zuijderwijk (Tata Steel Europe), as well as Tata Steel Europe and Cleveland-Cliffs Steel Corp. for project support, guidance, and materials.


## REFERENCES


1. O. Bouaziz, H. Zurob, and M. Huang, "Driving Force and Logic of Development of Advanced High Strength Steels for Automotive Applications," *Steel Research International*, vol. 84, no. 10, June 2013, pp. 937–947.
2. A. Karelova, C. Krempaszky, E. Werner, P. Tsipouridis, T. Hebesberger, and A. Pichler, "Hole Expansion of Dual-phase and Complex-phase AHS Steels - Effect of Edge Conditions," *Steel Research International*, vol. 80, no. 1, November 2009, pp. 71–77.
3. R. Stewart and R. Comstock "Hole Expansion Performance of Three High Strength Steels: Observation of Room Temperature Strain Aging Phenomena," *Steel Properties & Applications in conjunction with Materials Science & Technology 2021*, Columbus, OH, October 2021.
4. E. Atzema and P. Seda, "Effect of Zinc Coating and Time on Edge Ductility," *5th International Conference of Steels in Cars and Trucks 2017*, Amsterdam-Schiphol: Netherlands, June 2017.
5. N. Winzer, T. Schaffner, V. Kokotin, and R. Thiessen, "The Role of Hydrogen in Edge Cracking of Hot-Dip Galvanized AHSS Sheets," *Fourth International Conference on Metals & Hydrogen,* Ghent: Belgium, October 2022.
6. G. Dieter, "Strengthening Mechanisms,"*Mechanical Metallurgy*. McGraw-Hill Co., New York NY, 1961, pp. 201-203.
7. S. K. Paul, "Non-linear Correlation Between Uniaxial Tensile Properties and Shear-Edge Hole Expansion Ratio," *Journal of Materials Engineering and Performance.*, vol. 23, no. 10, October 2014, pp. 3610–3619.
8. J. A. Ronevich, J. G. Speer, and D. K. Matlock, "Hydrogen Embrittlement of Commercially Produced Advanced High Strength Sheet Steels*," SAE International Journal of Materials and Manufacturing*, vol. 3, no. 1, February 2010, pp. 255–267.
9. R. Scharf, A. Muhr, K.H. Stellnberger, J. Faderl, C. Holzer, and G. Mori, "Hydrogen Embrittlement of High Strength Steel Under in situ Corrosive Charging Conditions and Tensile Load," *Materials and Corrosion*, vol. 68, no. 1, January 2017, pp. 95–104.
10. S. Das, S. B. Singh, O. N. Mohanty, and H. K. D. H. Bhadeshia, "Understanding the Complexities of Bake Hardening," *Materials Science and Technology*, vol. 24, no. 1, January 2008, pp. 107–111.
11. B. S. Levy, M. Gibbs, and C. J. Van Tyne, "Failure during Sheared Edge Stretching of Dual-Phase Steels," *Metallurgical and Materials Transactions A,* vol. 44, no. 8, August 2013, pp. 3635–3648.
12. F. Li, H. Liu, W. Shi, R. Liu, and L. Li, "Hot Dip Galvanizing Behavior of Advanced High Strength Steel," *Materials and Corrosion*, vol. 63, no. 5, May 2012, pp. 396–400.
13. "Metallic Materials - Sheet and Strip - Hole Expanding Test," ISO 16630, 2019.
14. R. J. Comstock, D. K. Scherrer, and R. D. Adamczyk, "Hole Expansion in a Variety of Sheet Steels," *Journal of Materials Engineering and Performance*, vol. 15, no. 6, December 2006, pp. 675–683.
15. "Standard Test Methods for Tension Testing of Metallic Materials," ASTM E8-21, 2021.
16. B.W. Blesi, C. Smith, D.K. Matlock, and E. De Moor, "Bake Hardening Behavior of DP, TBF, and PHS Steels with Ultimate Tensile Strengths Exceeding 1 GPa," *SAE International Journal of Advances and Current Practices in Mobility*, SAE Technical Paper 2020-01-0536, April 2020.


 

17. H. Liu, F. Li, W. Shi, S. Swaminathan, Y. He, M. Rohwerder, and L. Lin "Challenges in Hot-Dip Galvanizing of High Strength Dual Phase Steel: Surface Selective Oxidation and Mechanical Property Degradation," *Surface & Coatings Technology*, vol. 206, no. 16, April 2012, pp. 3428–3436.

18. C.J. Smithells, W.F. Gale, T.C. Totmeier, "Diffusion in Metals," *Smithells Metals Reference Book (Eigth Edition)*, Elsevier Butterworth-Heinemann, Oxford, United Kingdom, 2004, pp. 13-78–13-80.

19. S.J. Lee, J.A. Ronevich, G. Krauss, and D.K. Matlock, "Hydrogen Embrittlement of Hardened Low-carbon Sheet Steel," *ISIJ International*, vol. 50, no. 2, February 2010 pp. 294–301.

 